22 kg/m^2, range 14.8–25) and to test for the inheritance of this frameshift mutation in the proband's family (Fig. 2). The mutation was not found in the control population. The mutation co-segregated with the severe obesity phenotype in the proband's family over three generations (lod score 1.5). All subjects bearing the mutation had a *Z* score at least four standard deviations above a normal BMI (ref. 9). The male carrier (III4) had a milder obesity, possibly suggesting a sex effect as seen in *Mc4r*-deficient mice. His BMI, however, was close to his sister's at age 20 years.

Our data indicate that a mutation in *MC4R* can cause a non-syndromic form of obesity with a monogenic dominant form of inheritance in humans.

Acknowledgements

We thank G. Bonhomme, A. Legall and E. Rocca-Serra for technical help and C. Dina for statistical advice. This work was supported by the Direction de la Recherche Clinique/Assistance Publique-Hopitaux de Paris and the Programme Hospitalier de Recherche Clinique (PHRC). We obtained consent from all family members and ethical permission was granted by the local ethics committee (CCPPRB, Hôtel-Dieu, Paris).

Christian Vaisse[1,2], Karine Clement[1,2], Bernard Guy-Grand[1,2] & Philippe Froguel[1,2]

[1]Institut de Biologie-CNRS EP10, Institut Pasteur de Lille rue Calmette 59000 Lille, France. [2]Laboratoire de Nutrition et Service de Médecine et Nutrition, Hôtel-Dieu place du Parvis Notre Dame 75004 Paris, France. Correspondence should be adressed to K.C. (e-mail: karine.clement@htd.ap-hop-paris.fr).

1. Comuzzie, A.G & Allison, D.B. *Science* **280**, 1374–1377 (1998).
2. Fan, W., Boston, B., Kesterson, V., Hruby, V. & Cone, R. *Nature* **385**, 165–168 (1997).
3. Huazar, D. *et al. Cell* **88**, 131–141 (1997).
4. Ollmann, M.M. *et al. Science* **278**, 135–138 (1997).
5. Seeley, R.J. *et al. Nature* **390**, 349 (1997).
6. Montague, C.T. *et al. Nature* **387**, 903–908 (1997).
7. Clément, K. *et al. Nature* **392**, 398–401 (1998).
8. Clément, K. *et al. Int. J. Obes. Relat. Metab. Disord.* **21**, 556–561 (1997).
9. Rolland-Cachera, M.F. *Eur. J. Clin. Nutr.* **45**, 13–21 (1991).
10. Stunkard, A. & Messick, S. *J. Psychosom. Res.* **29**, 71–83 (1985).

The premature ageing syndrome protein, WRN, is a 3′→5′ exonuclease

Werner syndrome (WS) is a human autosomal recessive disorder that causes the premature appearance of a partial array of disorders characteristic of old age[1,2]. These disorders include atherosclerosis, cancer, type 2 diabetes, osteoporosis, cataracts, wrinkled skin and grey hair, among other ailments. Cells cultured from WS subjects have a shortened replicative life span[3,4] and elevated rates of chromosome translocations, large deletions and homologous recombination[5,6]. The gene defective in WS, *WRN*, encodes a large RecQ-like DNA helicase[7] of 1432 aa. Defects in another human RecQ-like helicase, BLM, result in Bloom's syndrome[8] (BS), a genetic disorder that is quite different from WS. BS is manifested by short stature, neoplasia, immunodeficiency and high risk of cancer. Cells from BS subjects show an increase in sister chromatid exchanges.

DNA helicases can function in replication, repair, recombination, transcription or RNA processing. As WRN and BLM share no obvious homology outside the helicase domain, the non-helicase domains probably determine in which process each RecQ-like helicase participates, which provides the basis for the disparate cellular and organismal phenotypes that result from defects in these proteins.

Statistical sequence analyses showed subtle but significant similarities between

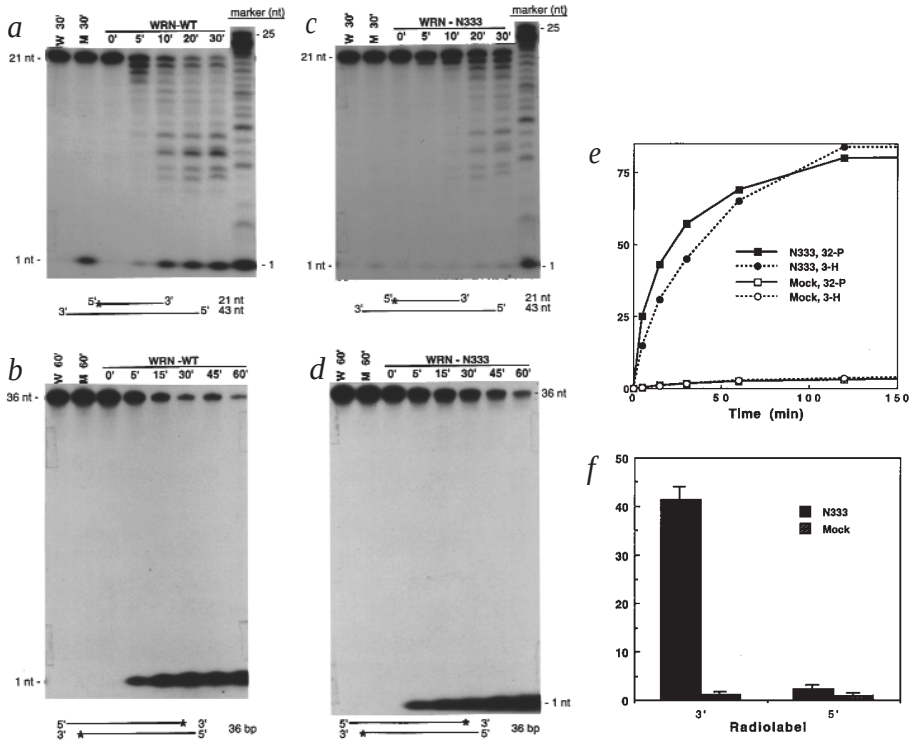

Fig. 1 Exonuclease activity of wild-type WRN and the N333 fragment. 6×his-tagged proteins were purified from baculovirus-infected insect cells using either nuclear (WRN, D82A, E84A, K577M, mock control) or cytosolic (N333, mock control) extracts. WRN, N-333, or mock proteins (10 ng, *a*,*b*; 5 ng, *c*,*d*) were incubated with 10,000 cpm of either a partial DNA duplex containing a 21-nt 5′ ^{32}P-labelled fragment annealed to an unlabelled 43-nt fragment (***a***,***c***) or a 36-bp DNA fragment ^{32}P-labelled at the 3′ end (***b***,***d***) in nuclease assay buffer (50 mM Tris-HCl, pH 7.5, 5 mM $MgCl_2$, 5 mM DTT, 0.1 mg/ml BSA) at 37 °C for the indicated intervals. Products were analysed on 20% polyacrylamide-8 M urea denaturing gels and visualized by autoradiography. M, mock; W, no protein addition. ***e***, N333 or mock proteins (20 ng) were incubated with a 374-bp DNA fragment labelled with ^{32}P at the 3′ end and ^{3}H at internal thymidine residues for the indicated intervals. The products were precipitated with 70% ethanol, and ethanol-soluble radioactivity was determined by scintillation counting. The activity is presented as percentage of input label (10,000 cpm ^{32}P; 6,000 cpm ^{3}H) that was soluble in 70% ethanol. ***f***, Equal amounts of 6×his-affinity purified N333 and mock proteins were resolved on a 8% non-denaturing polyacrylamide gel. The region containing N333 and a comparable region in the mock lane were excised, and the proteins eluted into nuclease buffer. The eluted N333 (20 ng) and mock proteins were incubated with 10,000 cpm of DNA substrates labelled to similar specific activities with ^{32}P at either the 5′ or 3′ end (*a*,*b*, respectively) for 1 h, and the activity was determined as in (*e*).

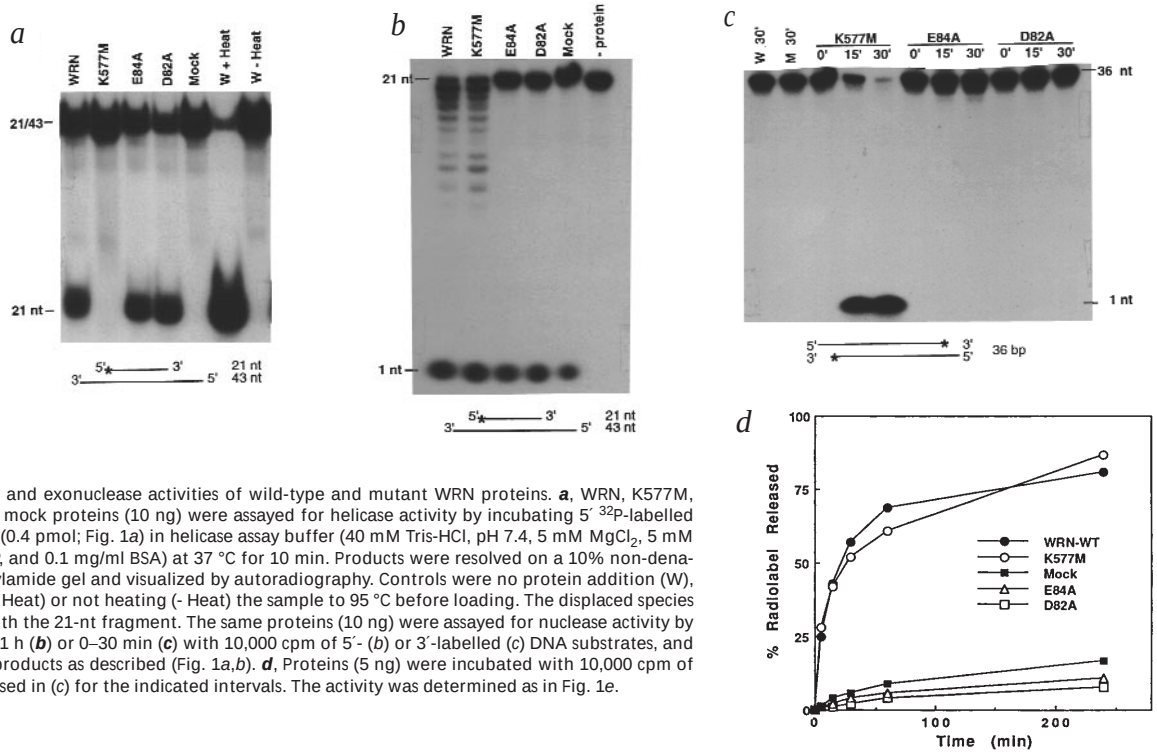

Fig. 2 Helicase and exonuclease activities of wild-type and mutant WRN proteins. ***a***, WRN, K577M, E84A, D82A or mock proteins (10 ng) were assayed for helicase activity by incubating 5′ ^{32}P-labelled DNA substrate (0.4 pmol; Fig. 1*a*) in helicase assay buffer (40 mM Tris-HCl, pH 7.4, 5 mM $MgCl_2$, 5 mM DTT, 1 mM ATP, and 0.1 mg/ml BSA) at 37 °C for 10 min. Products were resolved on a 10% non-denaturing polyacrylamide gel and visualized by autoradiography. Controls were no protein addition (W), and heating (+ Heat) or not heating (- Heat) the sample to 95 °C before loading. The displaced species co-migrated with the 21-nt fragment. The same proteins (10 ng) were assayed for nuclease activity by incubating for 1 h (***b***) or 0–30 min (***c***) with 10,000 cpm of 5′- (*b*) or 3′-labelled (*c*) DNA substrates, and analysing the products as described (Fig. 1*a*,*b*). ***d***, Proteins (5 ng) were incubated with 10,000 cpm of the substrate used in (*c*) for the indicated intervals. The activity was determined as in Fig. 1*e*.

WRN and several 3′→5′ exonucleases[9,10]. To test the prediction that WRN is an exonuclease, we produced tagged recombinant wild-type and mutant WRN proteins. Two mutants had amino-acid substitutions at either position 82 (D82A) or 84 (E84A), two of the five residues predicted to be critical for exonuclease activity[9,10]. A third mutant had a substitution at position 577 (K577M), which abolished WRN helicase activity[11]. The fourth mutant was an N-terminal fragment (aa 1–333; N333) containing the putative exonuclease domain, but lacking the helicase domain. A tagged 36-aa vector-derived peptide served as a negative control (mock).

Purified WRN and mock proteins were incubated with doubled-stranded DNA substrates. Wild-type WRN degraded a 5′ labelled substrate to a series of smaller, labelled products (Fig. 1*a*), and a 3′ labelled substrate to a single labelled product that migrated as a mononucleotide (Fig. 1*b*). Thus, WRN degraded DNA with 3′→5′ directionality. Although mock and full-length WRN preparations contained low levels of a contaminating 5′→3′ exonuclease, as shown by release of the 5′ label as a mononucleotide (Figs 1*a*,2*b*), 3′→5′ degradation was entirely dependent on WRN.

WRN exonuclease activity resided in the N terminus. N333, which was essentially free of contaminating 5′→3′ exonuclease, degraded 5′ and 3′ labelled substrates similarly to full-length WRN (Fig. 1*c*,*d*). When incubated with a 374-bp DNA fragment labelled at the 3′ end with ^{32}P, and internally with ^{3}H, N333 released most of both labels (Fig. 1*e*). Thus, the WRN exonuclease is capable of substantial DNA degradation. Consistent with 3′→5′ directionality, N333 released ^{32}P from 3′ ends more rapidly than ^{3}H from internal residues. In addition, gel-purified N333, which lacked contaminating nuclease activities, efficiently removed the 3′, but not the 5′, label when incubated with DNA substrates labelled at either the 3′ or the 5′ end (Fig. 1*f*).

Genetic evidence for WRN exonuclease activity was obtained by introducing point mutations at critical amino acids in the exonuclease domain (D82A and E84A). These mutants retained the wild-type level of helicase activity (Fig. 2*a*), but had little or no 3′→5′ exonuclease activity, using either a 5′ (Fig. 2*b*) or 3′ (Fig. 2*c*) ^{32}P-labelled substrate, and were indistinguishable from mock protein in this regard (Fig. 2*d*). The K577M mutant, in contrast, was devoid of helicase activity (Fig. 2*a*), as expected, but had 3′→5′ exonuclease activity comparable to that of wild-type WRN (Fig. 2*b*–*d*).

Our data indicate that WRN is indeed a 3′→5′ exonuclease. This activity resides in the N terminus, and is physically and functionally separable from the helicase activity. The identification of an exonuclease activity in WRN clearly distinguishes it from other human RecQ-like helicases, and may help explain the differences between WS and BS.

What are the functions of the WRN exonuclease *in vivo*? It may participate in recombination and DNA repair. Exonucleases are integral components of some recombination pathways[12], and WRN appears to have a role in recombination[5,6,13]. The finding that WS cells are hypersensitive to the DNA damaging agent 4-nitroquinoline-1-oxide[14] suggests a role for WRN in DNA repair. Finally, WRN is homologous to FFA-1 (replication focus-forming activity 1) in *Xenopus laevis*[15], raising the possibility that WRN may also be involved in DNA replication. In this context, the WRN exonuclease may provide 3′→5′ proofreading function to DNA polymerases that lack such activity. Whatever the case, an understanding of the functions of WRN exonuclease and their relationships to the other functions of WRN will lead to new insights into the molecular and cellular basis for WS and a subset of age-associated pathologies.

Acknowledgements

We thank S. Linn for valuable discussions and H. Asahara for technical advice. This work was supported by the National Institute on Ageing (grants AG11658 (J.C.); AG05776 (S.H.); AG14446 (J.O.)) and Department of Energy under contract DE-AC0376SF00098 to the University of California.

Shurong Huang[1], Baomin Li[1], Matthew D. Gray[2], Junko Oshima[2], I. Saira Mian[3] & Judith Campisi[1]

[1]Department of Cell and Molecular Biology, Lawrence Berkeley National Laboratory,

Berkeley, California 94720, USA. [2]Department of Pathology, University of Washington, Seattle, Washington 98195, USA. [3]Department of Radiation Biology, Lawrence Berkeley National Laboratory, Berkeley, California 94720, USA. Correspondence should be addressed to J.C. (e-mail: jcampisi@lbl.gov).

1. Martin, G.M. *Birth Defects* **14**, 5–39 (1978).
2. Goto, M. *Mech. Ageing Dev.* **98**, 239–254 (1997).
3. Martin, G.M., Sprague, C.A. & Epstein, C.J. *Lab. Invest.* **23**, 86–92 (1970).
4. Salk, D., Bryant, E., Hoehn, H., Johnston, P. & Martin, G.M. *Adv. Exp. Bio. Med.* **190**, 305–311 (1985).
5. Fukuchi, K., Martin, G.M. & Monnat, R.J. *Proc. Natl Acad. Sci. USA* **86**, 5893–5897 (1989).
6. Cheng, R.Z., Murano, S., Kurz, B. & Shmookler-Reis, R.J. *Mutat. Res.* **237**, 259–269 (1990).
7. Yu, C.E. *et al. Science* **272**, 258–262 (1996).
8. German, J. *Medicine* **72**, 393–406 (1993).
9. Main, I.S. *Nucleic Acids Res.* **25**, 3187–3195 (1997).
10. Mushegian, A.R., Bassett, D.E. Jr, Boguski, M.S., Bork, P., & Koonin, E.V. *Proc. Natl Acad. Sci. USA* **94**, 5831–5836 (1997).
11. Gray, M.D. *et al. Nature Genet.* **17**, 100–103 (1997).
12. Linn, S.M., Lloyd, R.S. & Roberts, R.T. *Nucleases* (Cold Spring Harbor Laboratory Press, New York, 1993).
13. Yamagata, K. *et al. Proc. Natl Acad. Sci. USA* **95**, 8733–8738 (1998).
14. Ogburn, C.E. *et al. Hum. Genet.* **101**, 121–125 (1997).
15. Yan, H., Chen, C.-Y., Kobayashi, R. & Newport, J. *Nature Genet.* **19**, 375–378 (1998).

Transcription of IAP endogenous retroviruses is constrained by cytosine methylation

Activation of the promoters of parasitic sequence elements (transposons and endogenous retroviruses) causes dysregulation of nearby cellular genes and induces new mutations *via* replicative transposition[1]. The most aggressive parasitic sequences extant in the mouse genome are the intracisternal A particle (IAP) retroviruses[2,3], which are normally transcriptionally silent. This could be due to the fact that the LTR regions of the 1,000–2,000 IAP proviruses in the mouse genome are heavily methylated in DNA of somatic tissues[2]. We determined the effect of induced demethylation on IAP provirus transcription in somatic tissues, and tested for demethylation in normal germ cells and preimplantation embryos to determine whether cytosine methylation could oppose provirus infiltration of the germ line.

IAP transcript levels are elevated 50–100-fold in mouse embryos deficient in DNA methyltransferase-1 (Dnmt1, encoded by the gene *Dnmt*; Fig. 1). Accumulation of transcripts from all major classes of IAP elements (class I, IΔ1and II; ref. 2) was observed, and IAP transcripts were present at high levels throughout the mutant embryos, as shown by *in situ* hybridization (Fig. 1*d*). These data confirm that demethylation of DNA activates IAP transcription in somatic tissues of mouse embryos, presumably through demethylation of LTR sequences.

It has been suggested that the genome is demethylated during preimplantation development, and again during gametogenesis, which might argue against a role for cytosine methylation in limiting the spread of parasitic sequences in the germ line[4]. The methylation status of IAP LTR sequences was evaluated in DNA isolated from purified primordial germ cells, 2,100 unfertilized oocytes, 800 blastocysts, epididymal sperm and midgestation embryos. IAP LTR sequences were heavily methylated at *Hpa*II (5′–CCGG–3′) sites in DNA from the oocyte, spermatozoon, blastocyst and midgestation embryo. IAP proviral DNA in primordial germ cells of embryonic day (E) 13.5 embryos was largely unmethylated at tested sites. *De novo* methylation occurs before meiosis in non-dividing prospermatogonia, but only after the pachytene stage of meiosis in growing oocytes (Fig. 2*a*,*b*). A small population of IAP LTR sequences was demethylated in blastocysts (Fig. 2, lane 8); this probably reflects general demethylation in the trophectoderm[5]. Demethylation of IAP DNA in primordial germ cells is not associated with high-level transcription of IAP proviruses. Primordial germ cells are migrating through the dorsal mesentery in E9.5 embryos, but elevated levels of IAP transcripts were not observed in the vicinity of this structure by *in situ* hybridization of wild-type embryos (Fig. 1*d*), nor did *in situ* hybridization show accumulation of IAP transcripts in genital ridges of E10.5 embryos (data not shown).

Primordial germ cells of both sexes are near the end of the proliferative phase at E13.5, and the interval during which the genome is both replicating and demethylated is short. This would minimize vulnerability to transposition, if IAP retroviruses require demethylation for transcription and passage through M phase for integration of newly synthesized viral DNA, as do nearly all other retroviruses[6]. Male germ cells of the mouse undergo only a few divisions as demethylated primordial germ

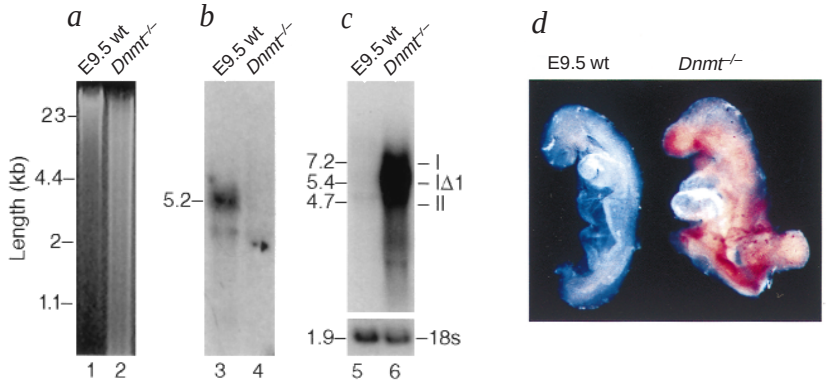

Fig. 1 Demethylation and transcriptional activation of IAP retroviruses in homozygous *Dnmt*$^{-/-}$ mutant mouse embryos. ***a***, Demethylation of genomic DNA. DNA from wild-type (lane 1) and *Dnmt*$^{-/-}$ mutant embryos (lane 2) was digested with the methylation-sensitive restriction endonucleases *Hpa*II and *Hha*I. Mean fragment sizes of mutant embryo DNA are lower than in the control. ***b***, Low levels of *Dnmt* mRNA in mutant embryos. Alternative splicing around the disrupted exon in the N allele of *Dnmt*$^{-/-}$ used in these studies allows the production of small (approximately 5% of wild-type) amounts of enzymatically active Dnmt1 protein[10]. ***c***, High-level expression of IAP RNA in *Dnmt*$^{-/-}$ embryos. The blot shown in (*b*) was stripped and probed with a IΔ1 IAP probe originally isolated from an IAP insertion allele of the *Axin* gene[11]. Densitometry indicated an approximately 50–100-fold increase in steady state IAP transcript levels. At bottom is the same blot probed for 18s rRNA to confirm equal loading. ***d***, *In situ* hybridization of wild-type and *Dnmt*$^{-/-}$ mutant embryos with an IAP probe. IAP transcripts are detected in all regions of the mutant embryos; the heart wall stains lightly due to its thinness.